

# Collection of Photoelectrons and Operating Parameters of CsI Photocathode GEM Detectors

B. Azmoun, A. Caccavano, Z. Citron, M. Durham, T. Hemmick, J. Kamin, M. Rumore, and C. Woody

**Abstract**—A study has been made of the parameters affecting the extraction and collection of photoelectrons from the surface of a CsI photocathode in a triple GEM detector. The purpose of this study was to optimize the photoelectron collection efficiency and GEM operating conditions for the PHENIX Hadron Blind Detector (HBD) at RHIC. The parameters investigated include the electric field at the surface of the photocathode, the voltage across the GEM, the electric field below the GEM, the medium into which the photoelectrons are extracted (gas or vacuum), and the wavelength dependence of the extraction efficiency. A small, calibrated light source, or “scintillation cube” was used to illuminate a GEM CsI photocathode with a known photon flux produced by the scintillation light from 5.48 MeV alpha particles in  $\text{CF}_4$ . The photoelectron collection efficiency was calculated by comparing the number of photoelectrons produced to the number collected at the GEM readout pad. Results are presented on the study of the parameters affecting the photoelectron collection efficiency and the construction and calibration of the scintillation cube.

**Index Terms**—GEM detectors, micropattern gas chambers, photocathodes, photodetectors, scintillation detectors, ultraviolet detectors.

## I. INTRODUCTION

THE quantum efficiency and photoelectron collection efficiency of CsI photocathodes has been studied by a number of authors [1]–[8]. However, the measurements have shown conflicting results, particularly regarding the maximum number of photoelectrons that can be extracted from a CsI photocathode surface into various gases and subsequently transported into the gain region of a GEM detector. This process is of great importance for the performance of the PHENIX Hadron Blind Detector (HBD), which uses CsI photocathode GEM detectors to detect Cherenkov photons produced by relativistic particles in a  $\text{CF}_4$  radiator in heavy ion collisions at RHIC [9]–[11]. The purpose of this study was to investigate the parameters affecting the photoelectron collection efficiency for CsI photocathode GEM detectors operated in pure  $\text{CF}_4$ , in order to better understand this process and to optimize the performance of the HBD.

Manuscript received January 01, 2009; revised April 02, 2009. Current version published June 17, 2009. This work was supported by the U.S. Department of Energy, Division of Nuclear Physics, under Prime Contract DE-AC02-98CH10886.

B. Azmoun, A. Caccavano, and C. Woody are with Brookhaven National Laboratory, Upton, NY 11973-5000 USA (e-mail: woody@bnl.gov).

Z. Citron, M. Durham, T. Hemmick, and J. Kamin are with Stony Brook University, Stony Brook, NY 11794 USA.

M. Rumore is with Woster Polytechnic Institute, Woster, MA 01609-2280 USA.

Color versions of one or more of the figures in this paper are available online at <http://ieeexplore.ieee.org>.

Digital Object Identifier 10.1109/TNS.2009.2020983

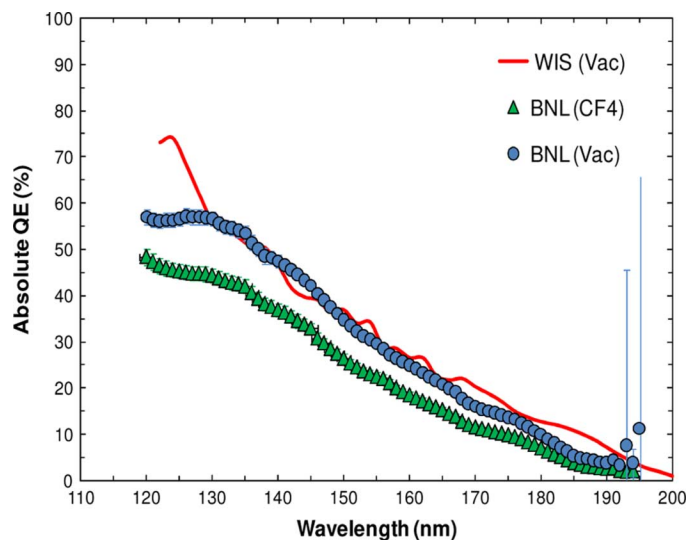


Fig. 1. The absolute quantum efficiency of several typical CsI photocathodes measured in vacuum and in pure  $\text{CF}_4$  in parallel plate collection mode. (Measurements performed at Weizmann Institute of Science [10] and Brookhaven National Lab.)

The HBD utilizes an array of triple GEM detectors where the top GEM has a  $\sim 300$  nm thick CsI photocathode layer deposited on its upper surface. A mesh electrode above this surface is used to control the field above the photocathode. It can be biased such that charge produced in the gap between the mesh and the top GEM is collected toward the GEM (Forward Bias) or by the mesh (Reverse Bias). The detector is operated in pure  $\text{CF}_4$ , where the  $\text{CF}_4$  acts as both the Cherenkov radiator and as the operating gas for the GEMs.

The main factor affecting the production of photoelectrons from the photocathode is the quantum efficiency. This can be measured in vacuum, in a parallel plate configuration, where all photoelectrons are collected by the mesh. Fig. 1 shows the quantum efficiency measured as a function of wavelength for some of our typical CsI photocathodes. The difference between the vacuum and  $\text{CF}_4$  measurements is believed to be due to backscattering processes within the gas and is further investigated in this study.

## II. PHOTOELECTRON COLLECTION EFFICIENCY

We define the photoelectron collection efficiency as the ratio of the number of photoelectrons that are collected and subsequently amplified in the gain region of the GEM detector to the number that are produced at the photocathode for a given quantum efficiency. We assume that the overall photoelectron collection efficiency can be factorized into two components: an *extraction efficiency* (EE) that gives the

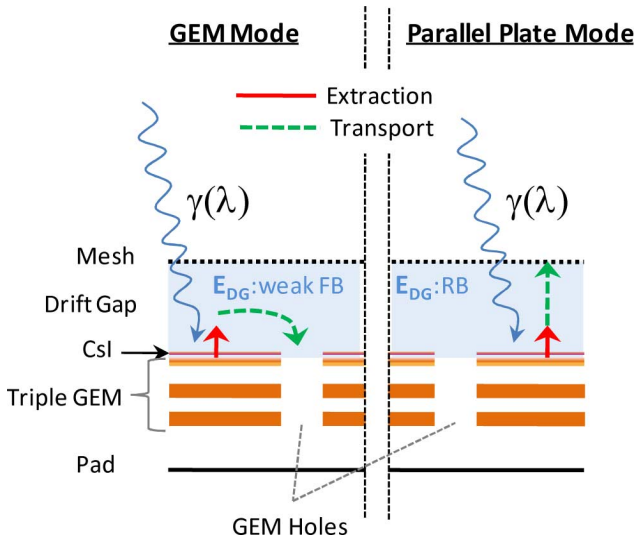


Fig. 2. Operation of a CsI photocathode GEM detector in normal GEM mode and in parallel plate mode. Red arrows indicate photoelectron extraction and green arrows indicate photoelectron transport. The drift gap field ( $E_{DG}$ ) is set to slight forward bias (FB) in normal GEM operation and reverse bias (RB) in parallel plate operation.

fraction of photoelectrons that are extracted from the surface of the photocathode without immediate recombination, and a *transport efficiency* (TE), which gives the probability that a photoelectron, once extracted, is successfully transported through the gas to the gain region of the GEM. The overall efficiency may then be expressed as the product of the two terms  $\varepsilon_{CE}(\mathbf{E}, \lambda) = \varepsilon_{EE}(\mathbf{E}, \lambda) \cdot \varepsilon_{TE}(\mathbf{E})$ . It is further hypothesized that the extraction efficiency depends on both the extraction field,  $\mathbf{E}$ , and on the wavelength of the incident photons,  $\lambda$ , whereas the transport efficiency only depends on the field.

Fig. 2 illustrates the role of each efficiency term in the operation of a CsI photocathode GEM. In normal GEM mode, photoelectrons are extracted off of the photocathode surface and transported to the holes of the GEM where they are amplified. In parallel plate mode, the photoelectrons are extracted from the surface and transported to the mesh where they are collected without amplification.

#### A. Extraction Efficiency

The photoelectron extraction efficiency in  $CF_4$  was measured in parallel plate collection mode using a VUV spectrometer (McPherson Model 234/302). The spectrometer was set to illuminate a photocathode with a constant flux of 160 nm photons both in vacuum and in  $CF_4$ . As seen in Fig. 3, the photoelectron extraction efficiency rapidly approaches the plateau value of 100% in vacuum as a function of the applied reverse bias field in the drift gap. However, in the presence of gas, the collection efficiency is reduced due to backscattering of the photoelectrons off of the gas molecules. Fig. 3 shows that in  $CF_4$ , the collection efficiency reaches a plateau value of  $\sim 80\%$  at a field of  $\sim 5$  kV/cm, which is approximately the magnitude of the field at the photocathode surface for a normally operating GEM. The measurement was done using both GEM photocathodes and solid planar photocathodes, which gave consistent results. In argon, the collection efficiency is much lower, and there is no plateau

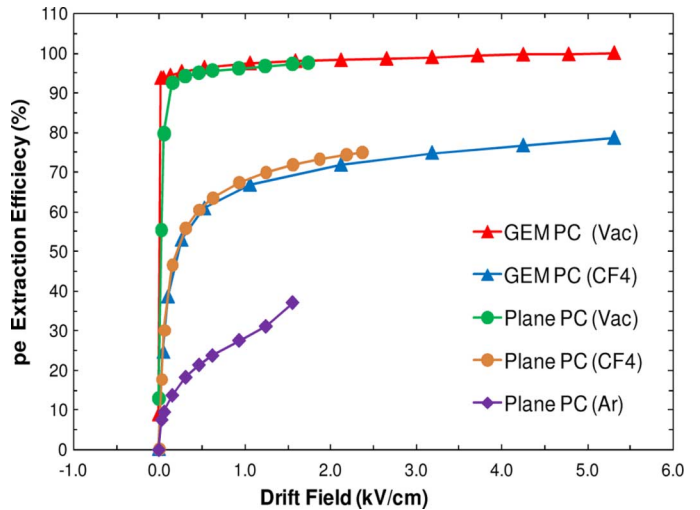


Fig. 3. Photoelectron extraction efficiency as a function of electric field in parallel plate collection mode for both GEM photocathodes (GEM PC) and planar photocathodes (Plane PC) in vacuum,  $CF_4$  and argon.

for fields less than 2 kV/cm. The higher efficiency in  $CF_4$ , compared to monatomic gases like argon, is due to its vibrational modes of excitation, which effectively reduces the probability for backscattering and recombination at low electron energies [5]–[7].

Fig. 4 shows that the same efficiency is measured for different drift gap distances, indicating that the loss of electrons takes place close to the photocathode surface (presumably over a distance of a few mean free paths), and is therefore not due to attachment or recombination of electrons during transport through the bulk gas volume (i.e.,  $\varepsilon_{TE} = 1$  and  $\varepsilon_{CE} = \varepsilon_{EE}$  in parallel plate mode). It should also be noted that the gas transmission was simultaneously measured by the spectrometer during these measurements and was determined to be greater than 99% at 160 nm, so any observed loss of photoelectrons in the gas is not due to absorption.

The processes of backscatter and transport losses and their effect on the photoelectron collection efficiency in  $CF_4$  and other gases has also been investigated using detailed Monte Carlo simulations by other authors [5]–[7]. They predict that the collection efficiency depends not only on the field, but also on the wavelength of the incident light. This has to do with the detailed electron scattering processes in the gas, but is mainly due to the vibrational excitation of  $CF_4$  molecules at low electron energies. These processes are described in detail in those references. Our measurements agree qualitatively with these predictions, as shown in Fig. 5, which indicates that the extraction efficiency decreases with increasing photon energy.

#### B. Collection Efficiency

The overall photoelectron efficiency was determined by illuminating a CsI photocathode triple GEM detector with a calibrated light source for which the emitted photon flux was known, and therefore the number of photoelectrons produced could be determined using the known quantum efficiency of the photocathode. The setup is shown in Fig. 6. The overall collection efficiency was then given by the ratio of the number

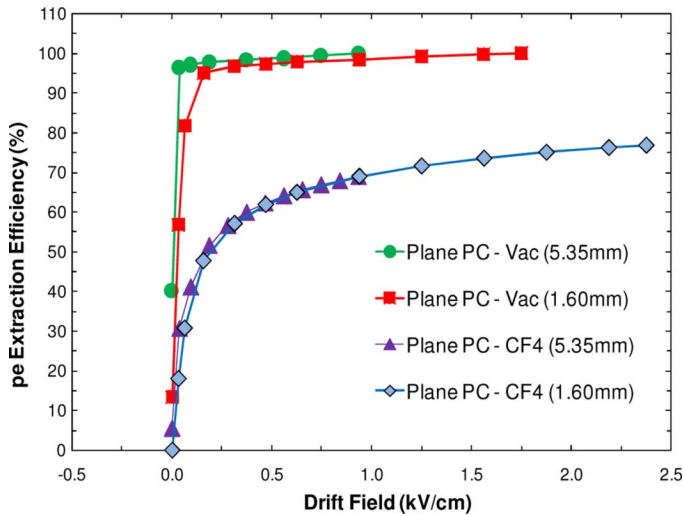


Fig. 4. Photoelectron extraction efficiency in vacuum and in  $\text{CF}_4$  for two different drift gap distances: 1.60 mm and 5.35 mm.

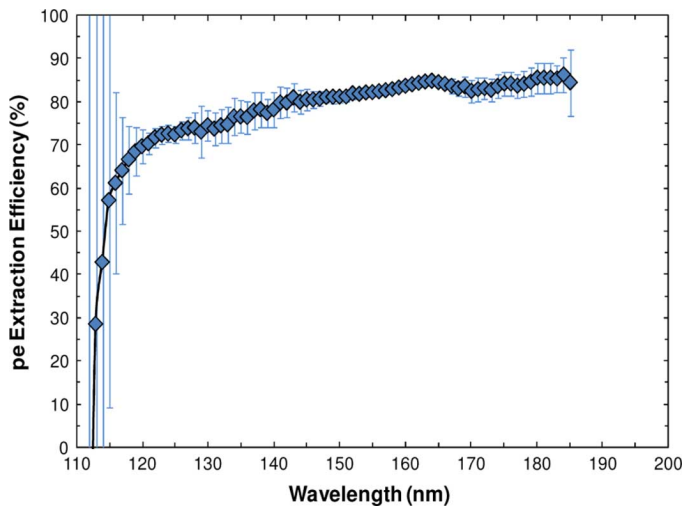


Fig. 5. Photoelectron extraction efficiency vs. incident photon wavelength, measured in parallel plate collection mode with a drift gap field of 5.3 kV/cm.

of photoelectrons contributing to the final GEM signal to the initial number produced:

$$\varepsilon_{\text{CE}} = \text{Npe}(\text{collected}) / \text{Npe}(\text{produced}).$$

Two independent methods have been utilized to determine  $\text{Npe}(\text{collected})$  and  $\text{Npe}(\text{produced})$ . The first involves calculating the mean of each pulse height spectrum and then determining the primary charge from the knowledge of the gain and preamp calibration. The second is a more sophisticated method that relies on an analysis of the shape of the pulse height spectrum and will be discussed below. In general, both methods yielded quite similar results and agreed to within a few percent.

A custom calibrated light source which exploits the scintillation emission band of  $\text{CF}_4$  centered at 160 nm ( $\sigma \sim 5$  nm) [12] was designed and constructed to provide a known flux of photons to illuminate the photocathode. A sketch of the light source, or “Scintillation Cube”, is shown in Fig. 6. Inside the cube,

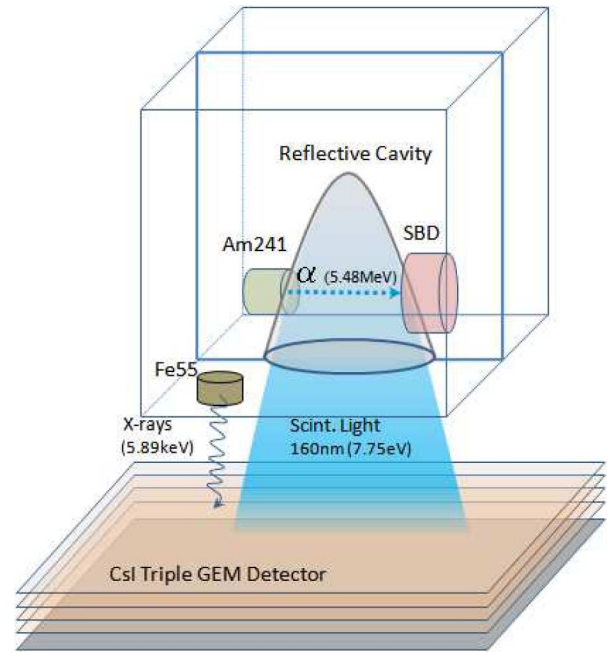


Fig. 6. Calibrated Light Source: “Scintillation Cube”, illuminating a CsI photocathode GEM detector.

$^{241}\text{Am}$  alpha particles traverse  $\sim 9$  mm of gas and produce scintillation light that emanates from a reflective cavity, thus providing a constant flux of 160 nm photons. Using a similar setup, we were also able to measure the absolute scintillation light yield in  $\text{CF}_4$ , which is reported elsewhere [13], [14]. A silicon surface barrier detector (SBD—Ortec Model BU-014-025-100) provides a signal to trigger on the alpha particle. In addition, the amplitude of the SBD signal provides information about the total energy deposited by the alpha in the gas. By initially determining the amplitude of this signal in vacuum, which corresponds to the full initial energy of the alpha (5.48 MeV), the SBD signal amplitude may be calibrated in terms of energy. The total energy deposited within the gas is then simply the initial energy of the alpha minus the energy deposited in the SBD.

The scintillation cube also includes an  $^{55}\text{Fe}$  source that simultaneously illuminates the GEM with 5.89 keV X-rays and allows a determination of the gas gain of the GEM. The GEM gain was calculated by taking the ratio of the total charge collected at the GEM pad, calibrated in terms of electrons, to the primary charge produced (on average 109 electrons for  $^{55}\text{Fe}$  X-Rays in  $\text{CF}_4$ ).

The absolute photon flux emanating from the scintillation cube was measured using a calibrated CsI photocathode PMT (Hamamatsu R6835). Both the quantum efficiency and the gain of the PMT were provided by the manufacturer. However, we also made our own measurements of these quantities. The quantum efficiency was measured using another PMT of the same type as a reference, and was found to match the factory value. The PMT gain was checked by obtaining the single photoelectron pulse height spectrum from the dark current noise and assigning the mean charge output to be that of a single photoelectron, which agreed fairly well with the factory gain.

A second method was also employed to determine the number of photoelectrons produced on the photocathode of the PMT. If

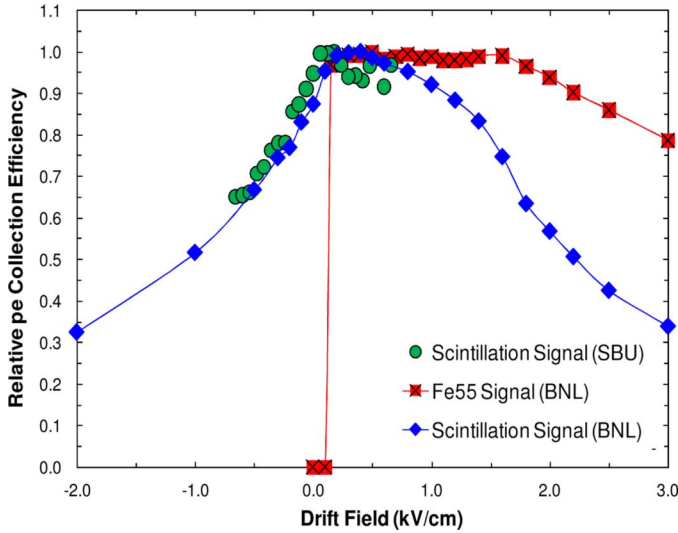


Fig. 7. Relative photoelectron collection efficiency vs. applied drift field. Crosses and diamonds were measurements done with a  $10 \times 10 \text{ cm}^2$  GEM at Brookhaven National Lab and circles were measurements done with a  $27 \times 22 \text{ cm}^2$  GEM at Stony Brook University.

one takes the ratio of events triggered by the SBD which produce no detected light in the PMT ( $P(0)$ ) to the total number of events within the pulse height spectrum, one can use the Poisson relation  $N_{pe} = -\log(P(0))$  to determine the mean number of primary photoelectrons.

The agreement between these two methods was excellent and yielded a value of  $N_\gamma = 9.6 \pm 0.5 \gamma/\text{MeV}$  for the flux emanating from the cube. The number of photoelectrons produced on the GEM CsI photocathode is then given by:

$$N_{pe}(\text{produced}) = N_\gamma * T_{\text{mesh}} * T_{\text{GEM}} * QE_{\text{CsI}(160 \text{ nm})}$$

where  $T_{\text{mesh}}$  and  $T_{\text{GEM}}$  are the mesh and GEM optical transparencies respectively, and  $QE_{\text{CsI}(160 \text{ nm})}$  is the quantum efficiency of the plane CsI photocathode measured at 160 nm in vacuum. Using our measured values for  $T_{\text{mesh}} = 0.80$ ,  $T_{\text{GEM}} = 0.83$ , and  $QE_{\text{CsI}(160 \text{ nm})} = 0.23$  gives:

$$N_{pe}(\text{produced}) = 6.3 \pm 0.3 \text{ pe/MeV.}$$

Fig. 7 shows the relative photoelectron collection efficiency versus the applied drift field. This efficiency is proportional to the total number of photoelectrons collected by the GEM. It shows a plateau for moderate positive drift fields (forward bias), and decreases for negative (or reverse) bias and large positive bias. The decrease for negative bias is evident from the fact that more electrons are pulled toward the mesh with increasing reverse bias field, while the decrease at large positive bias is due the fact that at very high forward bias, the field limits the efficiency with which electrons are extracted and transferred to the GEM holes. This is further discussed in Section III.

For the determination of the absolute overall collection efficiency, the drift field was set to  $+400 \text{ V/cm}$ , which is at the peak of the efficiency curve. However, we note that the HBD operates at a slightly negative drift field (typically  $\sim 100 \text{ V/cm}$ ), which introduces some additional loss in the collection efficiency. We

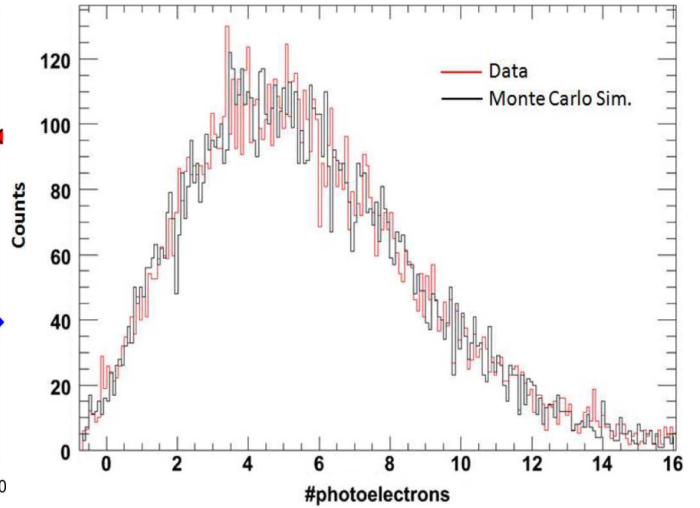


Fig. 8. Measured pulse height spectrum of scintillation light from the cube along with the Monte Carlo fit to the data to determine  $N_{pe}(\text{collected})$ .

also note that the efficiency for collecting  $^{55}\text{Fe}$  photoelectrons exhibits a flat plateau for positive drift gap fields, indicating that this efficiency is effectively 100%. This assumption was verified by another method that does not depend on the knowledge of the GEM gain, as discussed below.

The number of photoelectrons collected was also determined from an analysis of the shape of the GEM pulse height spectrum. This method assumes that the observed spectrum originates from a primary photoelectron distribution which follows Poisson statistics, which is then convoluted with a Polya distribution representing the gain fluctuations of the GEM detector, along with a Gaussian pedestal distribution. The shape of the pedestal distribution was measured directly from the experimental setup. The form of the Polya distribution is described in [15], and the value of the Polya parameter  $\theta$  used was 0.38. This value is the same as is used for similar operating conditions in wire chambers, as discussed in [14]. However, it should be noted that the Polya parameter only weakly influences the determination of the number of primary photoelectrons using this method (e.g., changes in  $\theta$  on the order 30% alter the value of photoelectrons by only a few percent.).

The analysis is carried out by generating a series of Monte Carlo simulated data in which the mean of the primary Poisson distribution is allowed to vary. By performing a Chi square analysis, the simulated data was then fit to the actual data in order to determine the best fit. Fig. 8 shows the measured spectrum compared with the fit, indicating excellent overall agreement. The mean of the primary photoelectron distribution corresponding to the best fit was then taken to be the actual  $N_{pe}$ .

The value of  $N_{pe}(\text{collected})$  determined using the mean method yielded a value of  $4.4 \pm 0.03$ , whereas the fitting method gave a value of  $4.0 \pm 0.05$ . The two results differed by more than their respective statistical errors, and the difference was taken to be a measure of the systematic error between the two measurements. A simple, non-weighted average was therefore taken as the best estimate of  $N_{pe}(\text{collected})$ , and an estimate of the total error was taken to be half of the difference between the two values, giving  $N_{pe}(\text{collected}) = 4.2 \pm 0.2$

pe/MeV. The photoelectron collection efficiency is then given by the ratio  $N_{pe}(\text{collected})/N_{pe}(\text{produced})$ :

$$\begin{aligned}\varepsilon_{CE}(E_o, = 160 \text{ nm}) &= 4.2 \pm 0.2 / 6.3 \pm 0.3 \\ &= 0.66 \pm 0.04.\end{aligned}$$

### C. Transport Efficiency

Using the value obtained above for the overall collection efficiency, one can determine the transport efficiency if the extraction efficiency is known. If we assume that the overall collection efficiency measured in parallel plate collection mode is the same as the extraction efficiency in GEM mode, then we can use the results given in Fig. 5 as an estimate of the extraction efficiency. At 160 nm, Fig. 5 gives a value for  $\varepsilon_{EE}(5 \text{ kV/cm}, 160 \text{ nm}) = 0.82 \pm 0.03$ , which corresponds to an electric field at the surface of the GEM of  $\sim 5 \text{ kV/cm}$  (note, however, that the *average* field in the drift gap is only  $\sim 0.4 \text{ kV/cm}$ ). This gives a value for the transport efficiency of:

$$\begin{aligned}\varepsilon_{TE}(E_o) &= \varepsilon_{CE}(E_o, 160 \text{ nm}) / \varepsilon_{EE}(5 \text{ kV/cm}, 160 \text{ nm}) \\ &= 0.80 \pm 0.08.\end{aligned}$$

The fact that the transport efficiency is less than one implies that there is a loss of photoelectrons after they have been extracted from the photocathode. This loss must therefore occur after the electrons have traveled several mean free paths away from the photocathode. The results shown in Fig. 4 rule out loss mechanisms such as attachment or recombination resulting from the traversal of photoelectrons through the bulk volume of gas. However, it is possible that the observed loss of photoelectrons could be due to a process similar to that caused by backscattering at extraction, namely, scattering of electrons back towards the photocathode during transport. As photoelectrons leave the photocathode and head toward the GEM holes, they remain quite close to the photocathode surface. As discussed below, many field lines (and hence photoelectron trajectories) are within only a few tens of microns from the photocathode, which is comparable to the mean free path for an elastic collision in  $\text{CF}_4$ . Hence, it is quite possible that additional photoelectrons are lost due to scattering and subsequent recombination at the photocathode along their path toward the GEM holes.

### III. EFFECTS OF THE ELECTRIC FIELD NEAR THE GEM HOLES ON THE COLLECTION EFFICIENCY

In order to better understand the electric field at the photocathode surface and the distribution of field lines that carry photoelectrons into the gain region inside the holes of the GEM, we developed a 3D model of the field the using Maxwell simulation program [16]. Fig. 9 shows a visualization of the field in the region of a hole for the reverse and forward bias mode of the HBD. The lines shown are simply trajectories of photoelectrons produced uniformly over the photocathode surface and do not represent the actual density of electric field lines. However, the model does demonstrate that the transport of photoelec-

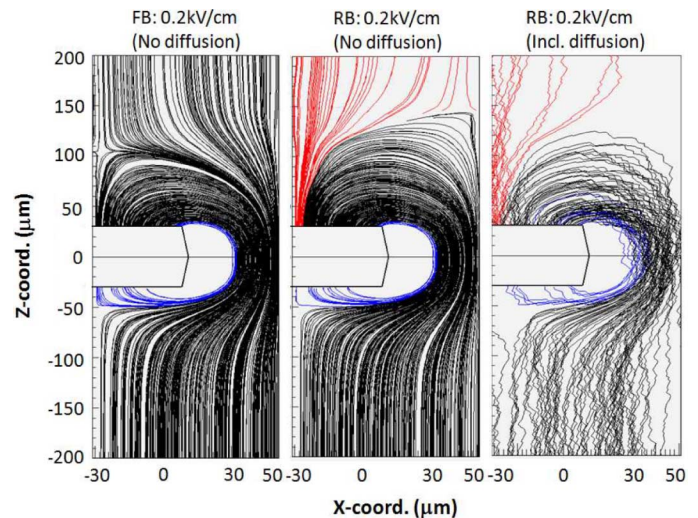


Fig. 9. Visualization of electric field lines in the vicinity of a GEM hole in forward bias mode (left), reverse bias mode (middle), and in reverse bias mode with the effects of diffusion included (right). Lines shown are trajectories of electrons emitted at the photocathode surface and do not indicate the actual density of electric field lines.

trons from the photocathode to the GEM holes takes place in a very small region above the photocathode ( $\sim 100 \mu\text{m}$ ), which could lead to further recombination at the photocathode as electrons undergo scattering along their trajectory. This effect will then result in a lower efficiency for collecting photoelectrons in GEM mode, compared to collecting photoelectrons from a photocathode operated in a parallel plate configuration.

Fig. 9 also shows the number of field lines originating on the top surface of the upper GEM that terminate on the mesh (indicated in red) and on the bottom surface of the top GEM (indicated in blue) in reverse bias mode. The field lines that go to the mesh result in a loss of photoelectrons at reverse bias, as shown in Fig. 7. In addition, Fig. 9 shows the field lines in the drift gap for forward bias. While at modest forward bias voltages, as shown in the figure, there is still a sizeable photoelectron collection region above the GEM, at very high forward bias, the collection region becomes very small and the photoelectron collection efficiency decreases, as observed in Fig. 7.

Having determined that the drift field strongly affects the photoelectron collection efficiency, we also investigated the effect of the field within the GEM hole and in the first transfer gap on the collection efficiency. This was studied by measuring  $N_{pe}(\text{collected})$  as a function of the applied voltage across the GEM, or effectively, as a function of the GEM gain. The results are presented in Fig. 10 and show that  $N_{pe}(\text{collected})$  is independent of the voltage across the GEM over a rather large range in gain. Similarly, in Fig. 11, the collection efficiency is unaffected by the potential across the transfer gap. However, it is apparent that additional effective gain may be obtained by increasing the transfer gap voltage while keeping the GEM potential constant.

### IV. SUMMARY

The photoelectron collection efficiency of a CsI photocathode triple GEM detector operating in pure  $\text{CF}_4$  has been measured.

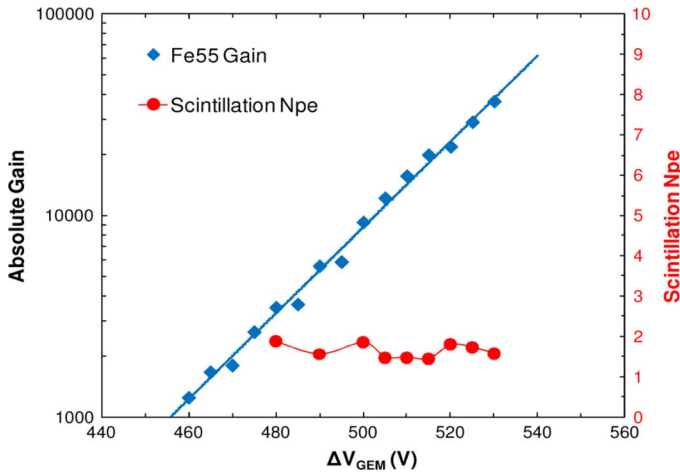


Fig. 10. GEM gain and scintillation signal ( $N_{pe}(\text{collected})$ ) as a function of voltage across the GEM.

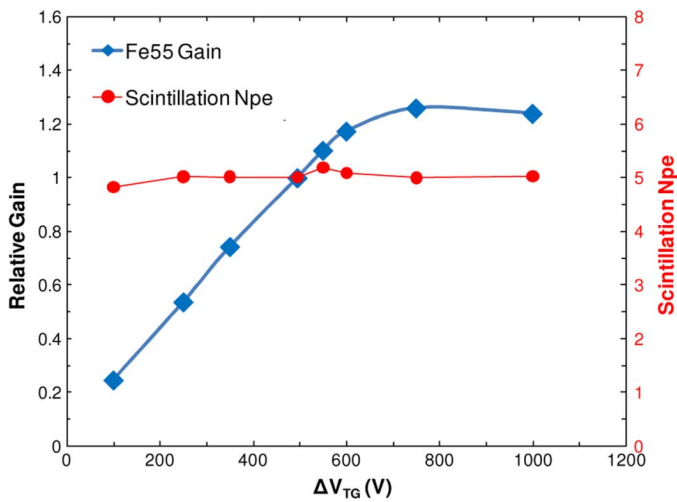


Fig. 11. Relative gain and scintillation signal ( $N_{pe}(\text{collected})$ ) versus voltage across the first transfer gap with the voltage across the GEM held constant.

The efficiency is assumed to factorize into two terms: an extraction efficiency that depends only on the probability to extract electrons from the photocathode surface without immediate recombination, and a transport efficiency that reflects the probability for transporting these photoelectrons to the GEM holes where amplification occurs. We find that under our normal GEM operating conditions, the extraction efficiency is  $0.82 \pm 0.03$  and the transport efficiency is  $0.80 \pm 0.08$ , leading to an overall

collection efficiency of  $0.66 \pm 0.04$ . The transport efficiency is considerably lower than in normal parallel plate operation of a CsI photocathode, and could be due to additional recombination losses of photoelectrons at the photocathode during transport. This process can be of great importance for photosensitive GEM detectors, such as the PHENIX HBD, where the maximum photoelectron collection efficiency is required in order to achieve optimum detector performance.

## REFERENCES

- [1] A. Breskin *et al.*, "Field dependent photoelectron extraction from CsI in different gases," *Nucl. Instrum. Methods Phys. Res. A*, vol. A367, pp. 342–346, 1995.
- [2] A. Di Mauno *et al.*, "Photoelectric backscattering effects in photoemission from CsI into gas media," *Nucl. Instrum. Methods Phys. Res. A*, vol. A371, pp. 137–142, 1996.
- [3] A. Buzulutskov *et al.*, "GEM photomultiplier operated in noble gas mixtures," *Nucl. Instrum. Methods Phys. Res. A*, vol. A443, pp. 164–180, 2000.
- [4] A. Breskin, A. Buzulutskov, and R. Chechik, "GEM photomultiplier operation in  $\text{CF}_4$ ," *Nucl. Instrum. Methods Phys. Res. A*, vol. A483, pp. 670–675, 2002.
- [5] J. Escada *et al.*, "A monte carlo study of backscattering effects in the photoelectron emission into  $\text{CH}_4$  and  $\text{Ar}/\text{CH}_4$  mixtures," in *Proc. IEEE Nuclear Science Symp. Conf. Rec.*, Rome, Italy, Oct. 16–22, 2004, pp. 559–563.
- [6] J. Escada *et al.*, "Photoelectron collection efficiency in mixtures of noble gases with  $\text{CF}_4$ ," in *Proc. Nuclear Science Symp. Conf. Rec.*, San Diego, CA, Oct. 29–Nov. 4 2006, pp. 1035–1038.
- [7] J. Escada *et al.*, "Photoelectron collection efficiency in  $\text{Xe}-\text{CF}_4$  mixtures," in *Proc. Nuclear Science Symp. Conf. Rec.*, Honolulu, HI, Oct. 27–Nov. 3 2007, pp. 585–589.
- [8] L. C. C. Coelho *et al.*, "Measurement of photoelectron collection efficiency in noble gases and methane," *Nucl. Instrum. Methods Phys. Res. A*, vol. A581, pp. 190–193, 2007.
- [9] A. Kozlov *et al.*, "Development of a triple GEM UV photon detector operated in pure  $\text{CF}_4$  for the PHENIX experiment," *Nucl. Instrum. Methods Phys. Res. A*, vol. A523, pp. 345–354, 2004.
- [10] Z. Fraenkel *et al.*, "A hadron blind detector for the PHENIX experiment at RHIC," *Nucl. Instrum. Methods Phys. Res. A*, vol. A546, pp. 466–480, 2005.
- [11] C. Woody *et al.*, "Prototype tests and construction of the hadron blind detector for the PHENIX experiment," in *Proc. Nuclear Science Symp. Conf. Rec.*, San Diego, CA, Oct. 29–Nov. 4 2006, pp. 1557–1561.
- [12] R. Gernhauser *et al.*, "Photon detector performance and radiator scintillation in the HADES RICH," *Nucl. Instrum. Methods Phys. Res. A*, vol. A371, pp. 300–304, 1996.
- [13] B. Azmoun *et al.*, "A measurement of scintillation in  $\text{CF}_4$  using GEM foils and a CsI photocathode," in *Proc. Nuclear Science Symp. Conf. Rec.*, Honolulu, HI, Oct. 27–Nov. 3 2007, pp. 623–626.
- [14] C. Woody *et al.*, "Collection of photoelectrons from a CsI photocathode in triple GEM detectors," in *Proc. Nuclear Science Symp. and Medical Imaging Conf. Rec.*, Dresden, Germany, Oct. 19–25, 2008, pp. 1316–1319.
- [15] J. Va'vra *et al.*, "Measurement of electron drift parameters for helium and  $\text{CF}_4$ -based gases," *Nucl. Instrum. Methods Phys. Res. A*, vol. A324, pp. 113–126, 1993.
- [16] 3D Maxwell, Ansoft Corporation, Pittsburgh, PA.